SPECTRAL POLISHING OF HIGH RESOLUTION IMAGING SPECTROSCOPY DATA

Daniel Schläpfer [a] and Rudolf Richter [b]

[a] ReSe Applications Schläpfer, Wil, Switzerland
daniel@rese.ch
[b] German Aerospace Center (DLR), Wessling, Germany
rudolf.richter@dlr.de

KEYWORDS: Atmospheric Correction, Polishing, Spectral Filter, Reflectance Artifacts Removal

ABSTRACT:

Imaging spectroscopy systems covering the visible to the short wave infrared range at wavelength resolutions below 10 nm are more and more used for research and for environmental applications. The compensation for influences of the atmosphere is well solved by inversion of radiative transfer codes as it is done by the ATCOR model or similar methods. However, spectral artifacts remain visible after the atmospheric correction. Current hyperspectral systems such as HySpex, AISA or APEX resolve the spectrum at sampling intervals down to 1-2 nm. Artifacts are usually visible in such data even after optimal correction for spectral smile distortions. The final correction for such artifacts is known as 'spectral polishing'. A variety methods of spectral polishing are tested on sample data sets of the Hyperion and the HySpex imaging spectrometer. Additionally, simulations on artificial data show trade-offs between information preservation and noise removal in the spectral polishing process. Based on this evaluation, recommendations are given on how to improve spectra by polishing techniques for both coarse and high resolution data. It is then shown, how such techniques are to be included as standard processing steps in higher level data processing chains.

1. INTRODUCTION

Current atmospheric correction packages are able to retrieve at-surface reflectance information from imaging spectroscopy data at a high level of accuracy ([Richter and Schläpfer, 2002], [Adler-Golden et al., 2004]). As the spectral resolution of these instruments has gradually been improved throughout the last years, spectral artifacts are more and more visible in the atmospherically corrected data. The reason for these high-frequency spikes and pseudo-absorptions are two-fold:

Type A: Systematic deviations are stemming from calibration or from data processing problems. They may be caused by inappropriate radiometric standards, by spectral miscalibration, by systematic errors in the description of the atmospheric absorption or from uncertainties in the solar reference spectrum.

Type B: Non-systematic (statistical) variations may be caused by the intrinsic variation of the atmosphere and the sun, the statistical photon shot noise, detector readout inconsistencies, so-called etalon-effects, or due to peculiar readout noise in the detector electronics.

The correction of these artifacts asks for system- and situation-specific techniques which are commonly known as 'spectral polishing'. This term could be defined as the removal of statistical noise and calibration artifacts in the spectral domain from atmospherically corrected imaging spectroscopy surface reflectance data. This polishing is necessarily to be done after atmospheric correction as high resolution artifacts occurring in the uncorrected at-sensor signatures are due to the atmospheric transmittance function.

In standard imaging spectroscopy at resolutions in a range of 10-30nm, the type A kind of errors are most prominent. Such types of errors may be best treated by radiometric filtering. This may be done using simple flat field or empirical line correction methods [Smith et al., 1987] or by using statistical analysis as implemented in the EFFORT [Boardman, 1998] polishing technique. These methods assume additional empirical gain/offset values for each spectral band to account for systematic errors. With the advance of pushbroom-type imaging spectrometry systems, however, the methods are to be improved in order to capture the variations of each detector pixel against its neighbours. Such corrections are also accounting for uncertainties of the solar spectrum which still are relevant at the scale of 5 to 10 nm (compare Fontenla [2009]). The respective difference of the 1997 standard spectrum by Kurucz [1995,1996] to the one of the most recent release of the solar spectrum of the quiet sun is given in Figure 1 .

The correction of type B spectral noise is only feasible by statistical filters. It is known from measurements that surface reflectance signatures below 2.5 µm hardly ever show narrow absorptions at resolutions below 10nm. Thus, the criterion of a 'good' spectrum at resolutions below 10nm is its smoothness in the spectral space. This smoothness may be achieved in various ways as described hereafter, from simple low pass filtering to advanced spectral transformation techniques. In this paper, we focus on airborne imaging spectrometry using modern instruments at resolutions below 5 nm. The goal is to show the various polishing options and to highlight advantages and disadvantages of some of them.

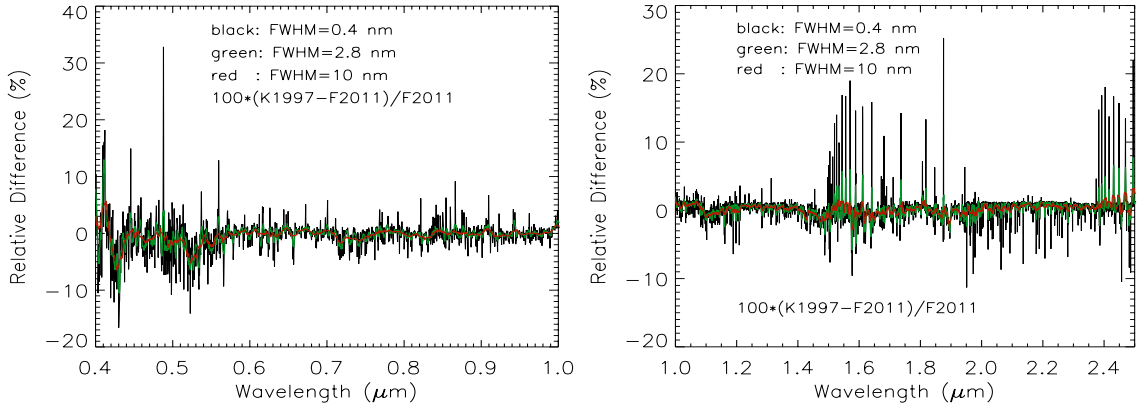

Figure 1: Difference of solar spectrum from Fontenla calibrated solar model ([Fontenla, 2009], 2011, pre-release) against Kurucz model [1995].

2. METHODS

The noise reduction in measured data is a task commonly done in various ways depending on the type of data. For surface reflectance spectra as inferred from airborne imaging spectrometers, two pecularities apply: first, the spectra are usually acquired contiguously , i.e., the data is not oversampled against the real data, but there might be gaps in strong atmospheric absorption regions (e.g., around 1400 nm, 1800 nm). Second, the real surface spectra are assumed to be continuous but still may contain relatively sharp natural absorption features in a range of 10-30 nm width. A good polishing algorithm should on the one hand be able to retain such sharp absorption features but on the other hand it should remove all non-natural spikes and pseudo-absorptions from the spectra. Hereafter, a compilation of possible methods to remove such artifacts is given; the first two methods deal with spectral noise of type A whereas the other methods are referring to non-systematic noise of type B.

2.1 Empirical Line Correction

The empirical line method may be used as a simple atmospheric correction routine and leads to acceptable surface reflectance results, specifically for non-calibrated imaging systems. Principally, there are two ways to apply the empirical line approach. The original idea was to use known surface reflectance spectra and to find an empirical relationship between the surface spectra and the at-sensor radiance values [Roberts et al., 1985]. An improved method was to use spectral mixture analysis to find the potential spectral shapes occuring in the images. All remaining signatures after mixing the real spectra are then attributed as noise and an empirical line may be applied to characterize these offsets. This routine was first described by Smith et al. [1987]. The disadvantage of this method is that signatures of non-common materials will be attributed to the noise fraction and would be filtered out from the imagery.

2.2 Smile Correction

Spectral smile is a non-uniformity of the across track spectral position of all pixels, typically occuring in pushbroom-type imaging spectrometers [Nieke et al., 2008]. Such spectral inconsistencies lead to artifacts, which are most prominently visible at the edge of sharp atmospheric absorption features (e.g., at the 760 nm oxygen band). Its operational correction needs to be done within the atmospheric correction software and has operationally been implemented in the current ATCOR codes [Richter et al., 2011]. This type of correction is a prerequisite to further polishing as it removes known calibration problems of the system.

2.3 Radiometric Polishing

Radiometric polishing assumes that a linear systematic bias is on top of the signal for each detector element. The origin of this linear function is not necessarily known. It is assumed that the offset depends on the signal strength as a multiplicative behaviour as it would occur with atmospheric transmittance values or radiometric gain miscalibration. Thus, a gain and an offset value are found for each detector element by evaluating the relation between the difference of the reflectance to the linearly interpolated reflectance on a 3-detector-pixel basis (optionally in both, spectral and spatial dimensions). A linear fit yields the coefficients per spectral band *j* for correction as:

$$\overline{\rho_{i,j}} = \text{interp}(\rho_{i,j-1}, \rho_{i,j+1}) \,, \qquad \text{and there from:}$$

$$\Delta\rho_{i,j} = \overline{\rho_{i,j}} - \rho_{i,j} \;\text{ and }\; (a,b)_j = \text{linfit}(\overline{\rho_{i,j}}, \Delta\rho_{i,j}) \qquad (1)$$

The corrected signal is then given as:

$$\rho^*_{i,j} = \rho_{i,j} + a_j + b_j \cdot \overline{\rho_{i,j}} \qquad (2)$$

For pushbroom-type sensor systems, this kind of radiometric adjustment has to be done carefully as the statistics of individual detector pixels may not be as representative as for whiskbroom imagery. Such methods have been successfully applied to various

whiskbroom systems (e.g. by the EFFORT routine [Boardman, 1998] as implemented in ENVI™ [ITTVis, 2011]), whereas the use on pushbroom systems is not yet well established due to reproducibility limitations. Gao et al. [1998] proposed a similar method which uses a cubic spline interpolation in order to get the empirical correction gain factors for the AVIRIS whiskbroom instrument, whereas Guanter et al., [2004] used a spectral mixture technique to find gain and offset residuals in CHRIS imagery

2.4 Low Pass Filter

A low pass filter is implemented as a moving average of the spectral bands with a typical window size of 3 to 7 spectral bands. The spectral bands are convolved to a symmetric kernel which is centered to the output band and which averages the respective bands. Further refinements of the method include the ability to decrease the low pass filtering strengths with the convolution kernels [0.17,0.66,0.17] and [0.25,0.5,0.25] respectively for filter sizes 1 and 2, respectively. Low pass filtering with kernel sizes larger than 7 bands reduces the information in the imagery substantially and has not been further used in this analysis.

2.5 Derivative Filter

A further type of filter is the derivative filter, which searches for the first derivative on either side of the spectral band to be polished. The two derivative lines are then evaluated at the position of the spectral band as an average of the two extrapolates. The band itself may optionally be included for filtering or may be completely replaced by the average extrapolate of the adjacent bands. First coefficients *(a,b)* are calculated as a linear fit on both sides of the spectral band *j* as:

$$(a,b)_{j,1} = \mathrm{linfit}(\lambda_{j-n:j-1}, \rho_{j-n:j-1}), \qquad \text{and} \qquad (a,b)_{j,2} = \mathrm{linfit}(\lambda_{j+1:j+n}, \rho_{j+1:j+n}) \tag{3}$$

There from the interpolated value is found with or without inclusion of the band itself as:

$$\rho_{j,filt} = \frac{a_{j,1} + \lambda_j b_{j,1} + a_{j,2} + \lambda_j b_{j,2}}{4} + \frac{\rho_j}{2} \quad \text{or} \quad \rho_{j,filt,adj} = \frac{a_{j,1} + \lambda_j b_{j,1} + a_{j,2} + \lambda_j b_{j,2}}{4} \tag{4}$$

The advantage of this type of filter is the preservation of absorption features, but it may also lead to a broadening of sharp features.

2.6 Savitzky-Golay Filter

The Savitzky Golay Filter [Savitzky and Golay, 1964] is an early numerical practice for the filtering of spectral data. It mimicks a polynomial interpolation of the data and transforms this kind of interpolation into a filter kernel. Usually, a 4th degree polynomial is selected for the filtering. It was originally used for very high resolution spectra with filter sizes above 10. Thus, its use is not optimal for medium to coarse resolution imaging spectroscopy at resolutions of 5-10 nm as specific spectral features may get lost. The advantage of this method is an efficient implementation whereas the disadvantage is the assumption of equally-spaced spectral bands for the convolution kernel. A validation of this technique is shown by Vaiphasa [2006].

2.7 MNF Transformation

The maximimum noise fraction transformation [Green et al., 1988] transforms the image with respect to its inherent noise. After ordering the resultant images, the noise components appear in the least significant bands and may be omitted. For this analysis, the MNF transformation as implemented in the ENVI™ software package [ITTVis, 2011] has been used. For the back-transformation, about one third of the most prominent spectral bands have been used whereas the remaining bands were deleted.

2.8 FFT Transformation

The fast Fourier transformation may be applied in the spectral domain onto a spectral image cube. High frequency signals are then to be eliminated before applying the back transformation. The resultant image shows considerably smoothed spectra. This kind of filtering is not very common to imaging spectroscopy as it assumes regular, ideally periodic signals in the spectral data. However, the spectra generally show almost arbitrary shapes which are not very well handled.

3. EXPERIMENTAL DATA ANALYSIS

For the intercomparison of the various polishing techniques, two types of data were used: a synthetic data set with variable noise on top of artificial spectra is first created. Secondly, subsets of selected Hyperion and the HySpex imaging spectrometer data have been taken.

3.1 Synthetic Data

The synthetic data was created on the basis of 12 spectra containing 50 spectral bands each as displayed in Figure 2. These spectra have been arranged in pseudo-image cube dimensions of 120 x 100, where additive noise is added in 'across-track' direction such that it reaches a maximum amount of 50 digital numbers (corresponding to a worst-case SNR of about 5). This synthetic data does not include systematic errors. Thus, the application of radiometric polishing techniques or empirical line methods is not feasible. The data have been treated with the above-mentioned statistical noise removal methods. Low pass filtering was limited at a maximum of

5 spectral bands, derivative polishing was done with up to 5 spectral bands on either side and the Savitzky-Golay filter was applied on the data on up to 8 spectral bands. For the MNF-Transformation a number of 20 MNF bands have been retained before applying the back-transformation. The same number of spectral bands were also omitted in the FFT transformed imagery.

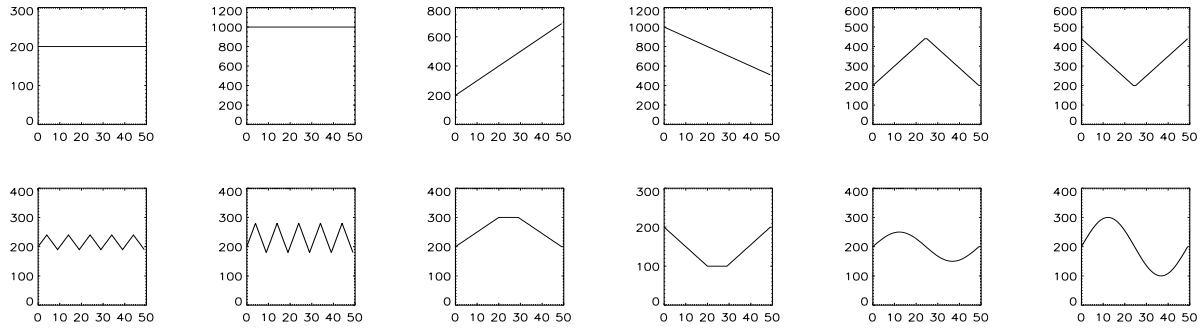

Figure 2: The 12 artifical spectra used for the synthetic data cube.

3.2 Hyperion Data

The spaceborne Hyperion imaging spectrometer [Pearlman et al., 2001] was the first truly operational imaging spectrometer in space offering the full VIS/NIR/SWIR spectral range at a spectral sampling interval of 10 nm. The ground sampling distance is approximately 30m with 256 across track pixels. Unfortunately, users had to deal with calibration and noise issues in the data throughout the lifetime of this sensor, but on the other hand this makes the sensor well suited for testing spectral polishing routines. The selected data set was acquired on November 11th, 2009 at the border between Texas and Louisiana (Sabine River area). A subset of the data after the first atmospheric correction step is shown in Figure 3 (left). Strong striping effects as well as some vignetting towards the edge of the detector is visible which are not the topic of this paper, however. The data has been reduced to a set of 167 'useful' spectral bands omitting the bands at the edges of the detectors and some bands in the water vapor absorption regions which are dominated by noise.

3.3 HySpex Data

The HySpex VNIR-1600 instrument [NEO, 2011] is measuring the spectral signature of the surface with 1600 across track pixels with a total FOV of 16.8°. HySpex scans at high spectral resolution in the VNIR spectral range between 408 and 985 nm in 160 spectral bands (i.e., ~3.5 nm spectral resolution). The instantaneous field of view is ~0.19mrad across track and 0.38mrad along track, corresponding to ~30cm*60cm pixel size for the given low altitude. The data was acquired at low illumination conditions in Norway on July 16th, 2007. As the data also is affected by a significant smile effect, the atmospheric correction first is done considering the smile as obtained from the imagery [Richter et al. 2011]. Both, radiometric and statistical spectral polishing techniques are then applied to this data set. Last but not least, the MNF transformation is tested and checked against the other methods.

Figure 3: Subset of the test data sets: Hyperion (left) and HySpex (right).

4. RESULTS

The intercomparison of the various polishing methods was first done on the synthetic data as this allows to get quantitative results in a well-defined way. The best ranking methods are then tested on the real data in order to check the applicability with real world instruments. The validation of the real data is only done on the basis of visual inspection and interpretation as no reliable ground reference information is available for these data sets.

4.1 Results on Synthetic Data

All statistical methods as described in Section 2 have been applied to the synthetic data set. The validation is done on the statistics by taking the standard deviation of the difference between the original spectrum and the filtered spectrum as a measure. Ideally, this standard deviation would be zero, but for the whole test image, it was between 8 and 12 DNs. The improvements of the filtering techniques were significant in most cases. It could be shown that the signals get worse if the low pass filter size box is four and more. The derivative filter was best when using 2-3 adjacent pixels to calculate the derivatives (compare Figure 4, which shows the mean, the minimum and the maximum standard deviation of the 50 spectral bands). The Savitzky-Golay filter (not shown in figure 4) performs on the same level of accuracy as the derivative filter, whereas FFT filtering leads to overcorrections, specifically for the test spectra with sharp absorption features. The EFFORT radiometric correction does not improve the results (as expected) because it is meant for systematic noise only. The clearly best performing method for the synsthetic data was the MNF correction.

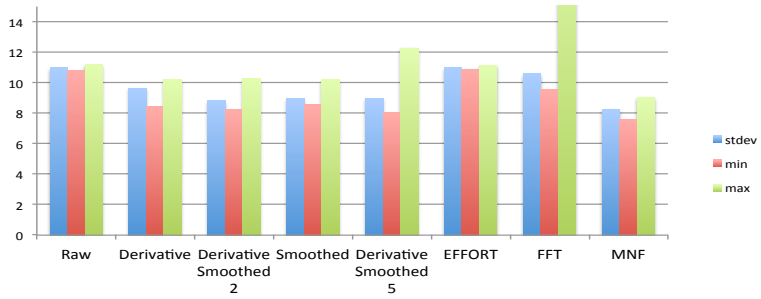

Figure 4: Statistical analysis of various filter techniques in comparison to unfiltered synthetic spectra (vertical axis are arbitrary digital numbers DN).

Visual inspection proves the finding from the statistical analysis. The MNF transformation reconstructs the original spectra in the most accurate way of all tested methods, whereas the derivative filters still did not preserve the features such accurately (compare Figure 5). Bands 1-9 and 41-50 are omitted in Fig. 5 as the edges of the spectra are not representative for the boxcar-filtering type algorithms.

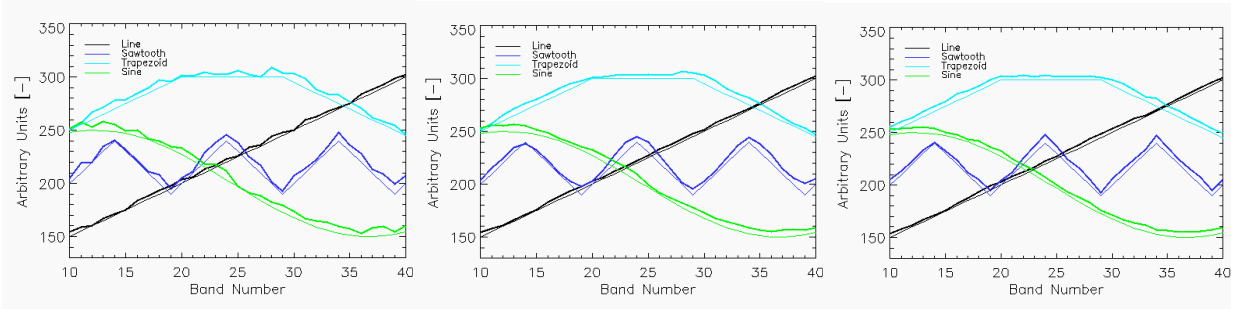

Figure 5: Effects of derivative filtering in comparison to MNF filtering (the smoother curves belong to MNF).

4.2 Hyperion Results

Some selected spectra of the Hyperion atmospheric correction are shown in Figure 6. The data has been first corrected for spectral smile in the atmospheric correction procedure which results in 'raw' surface reflectance values displayed in the first graphs of the figure. As this data still shows considerable systematic errors, the radiometric polishing is applied first. Attempts to use the MNF filtering in a second step did not improve the data as expected – some artifacts in the data are still too strong and are therefore not suppressed sufficiently through the MNF filter (not shown in Fig. 6). Therefore, the derivative low pass filter with a window size of 2 bands on either side and a factor of two for smoothing is applied. Note that this kind of moving average introduces new artifacts in the data at the edge of the omitted spectral bands of the water vapor absorption region.

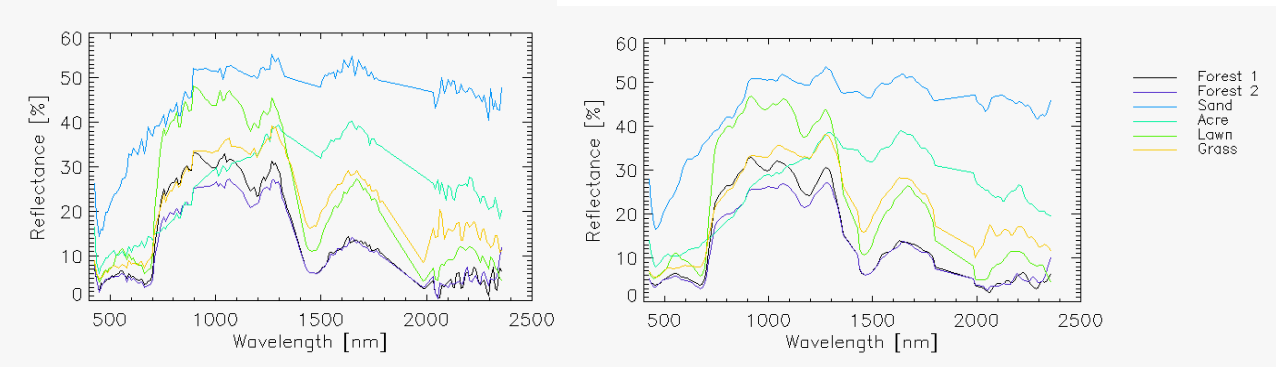

Figure 6: Hyperion atmospheric correction (left) and polishing results from radiometric polishing and derivative filtering (right).

4.3 Results on HySpex data

The similar procedures as with Hyperion were applied on HySpex data. As the data quality of this system is better than the one of Hyperion, no spectral smile needs to be considered in the atmospheric correction. The retrieved surface reflectances show still quite some noise towards the edges of the detector's spectral coverage. When trying to apply the radiometric filter, no improvement is visible. This leads to the conclusion that the remaining noise is non-systematic. The effects of the various filters are compared visually (see Figure 7). The derivative filter retains most of the features, but there remains still some noise in the data. The MNF transformation on the other hand produces quite smooth spectra in the regions where such characteristics are expected. However it seems that some features have been removed which shouldn't, and other unwanted spikes are still remaining in the data. The Savitzky-Golay filter as shown in the second row shows very promising results as it retains most of the features while the noise is well removed. Only at filter sizes above 6, the data seems to be too strongly smoothed against the original spectra.

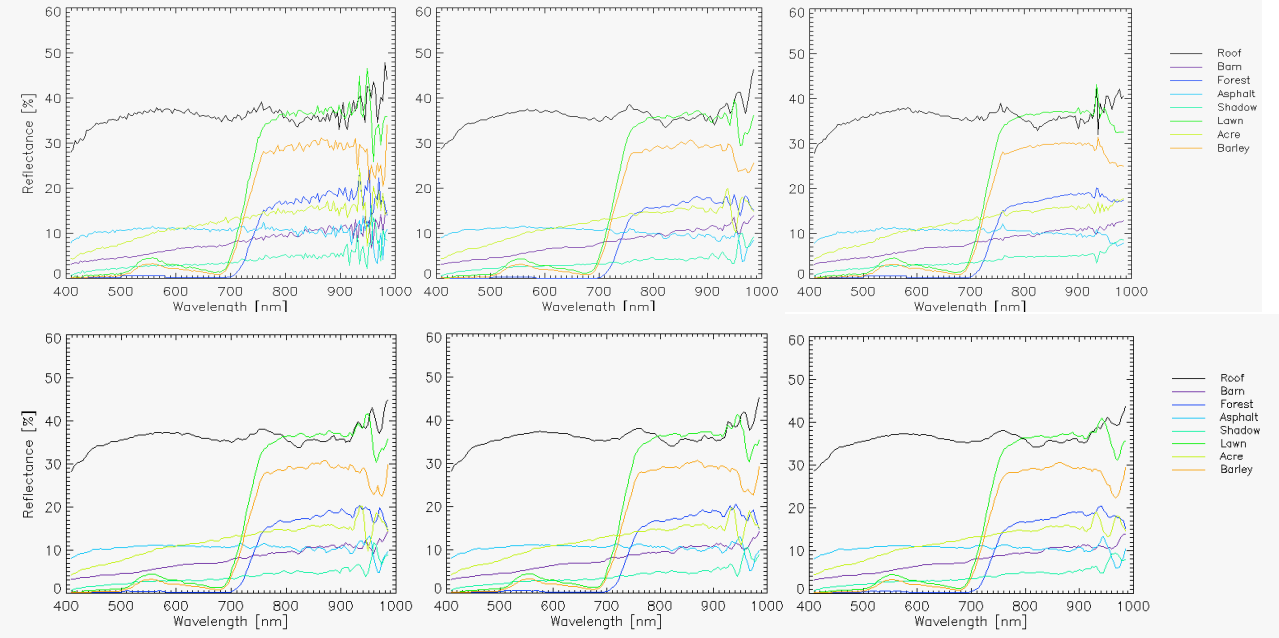

Figure 7: HySpex test data polishing: top-left: raw atmospheric correction; top-middle: derivative filter and slight low pass filter; top-right: MNF filter, bottom-left: SAVGOL-5, bottom-middle: SAVGOL-6, bottom-right: SAVGOL-8.

5. CONCLUSIONS

A broad variety of spectral polishing techniques has been applied to both synthetic and real imaging spectroscopy data. Concluding from the synthetic spectra, the MNF filtering technique proved to be well performing. Furthermore, the statistics showed that spectral smoothing should not go beyond a number of 5 spectral bands. However, the MNF rotation did not convince for the real data. The reason might be that the artifical data contains inherent regular patterns which can be well caught by the MNF rotation whereas non-sytematic features as in real data may be mathematically misinterpreted. For the Hyperion data, the importance of applying both smile correction and radiometric polishing has been shown. On this type of coarse spectral resolution data, the derivative smoothing appeared to be the best performing method for this type of broad band imagery.

For the spectrally higher resolved HySpex imagery, the advantage of the Savitzky-Golay method could be shown over the other methods investigated. This is not such surprising as this method has explicitly been defined for contiguous high resolution instruments. Further validation needs to be done in comparison to ground measurement spectra, however.

The importance of spectral polishing as part of a standard processing chain has been shown in this short analysis. It has to be noted that a polishing strategy needs to be defined for each sensor system separately as the types of noise may differ between the various systems due to resolution and calibration differences. Applying an appropriate standard filter will lead to improved spectra and will help to increase the usability of surface reflectance spectra from all kind of imaging spectroscopy instruments.

References

Adler-Golden, S., M. Matthew, L. Bernstein, R. Levine, A. Berk, S. Richtsmeier, P. Acharya, G. Anderson, G. Felde, and J. Gardner 1999. Atmospheric correction for short-wave spectral imagery based on MODTRAN 4, In: *Proc. SPIE, Imaging Spectrometry V*, vol. 3753, p. 61-69.

Boardman J.W., 1998. Post-ATREM Polishing of AVIRIS Apparent Reflectance Data using EFFORT: a Lesson in Accuracy versus Precision. In: *Summaries of the Seventh JPL Airborne Earth Science Workshop*, JPL Publication 97-21, Vol. 1, p. 53.

Fontenla J., W. Curdt, and M. Haberreiter, "Semiempirical Models of the Solar Atmosphere. III. Set of Non-LTE Models for Far-Ultraviolet/Extreme-Ultraviolet Irradiance Computation," The Astrophysical Journal, 2009.

Gao B.-C., M. Liu and C.O. Davis 1998. A New and Fast Method for Smoothing Spectral Imaging Data, In: *Summaries of the Seventh JPL Airborne Earth Science Workshop*, JPL Publication 97-21, Vol. 1, pp. 131-140.

Green A. A., M. Berman, P. Switzer, and M. D. Graig. 1988. A transformation for ordering multispectral data in terms of image quality with implications for noise removal. *IEEE Transactions on Geoscience and Remote Sensing*, vol. 26, no. 1, pp. 65-74.

Guanter L., L. Alonso, and J. Moreno, 2004. Atmospheric Correction of Chris/Proba Data Acquired in the Sparc Campaign. In: *Second Chris Proba Workshop*, vol. 578, p. 9.

ITT Vis, 2011. *ENVI Software - Image Processing & Analysis Solutions*. Version 4.8, at http://www.ittvis.com, (accessed 4/26/2011).

Kurucz R. L., and Bell, B. 1995. *Kurucz CD-ROM*, Cambridge, MA: Smithsonian Astrophysical Observatory, April 15.

Kurucz R. L., 1996. Model Stellar Atmospheres and Real Stellar Atmospheres. In: *Proceedings of the Vienna workshop on Model, Atmospheres and Spectrum Synthesis*, July 1995, ASP Conference, Series 108, pp. 18.

Nieke, J., D. Schläpfer, F. DellEndice, J. Brazile, and K. I. Itten, 2008. Uniformity of Imaging Spectrometry Data Products, *IEEE Transaction on Geoscience and Remote Sensing*, 46(10), 3326-3336.

Norsk Elektro Optikk AS, 2011. *HySpex HyperSpectral Cameras - HySpex VNIR-1600*. at http://www.hyspex.no, (accessed 4/26/2011)

Pearlman, J., S. Carman, and C. Segal, 2001, Overview of the Hyperion imaging spectrometer for the NASA EO-1 mission, in IEEE *Proc. IGARSS*. pp. 3.

Richter, R., and D. Schläpfer, 2002. Geo-atmospheric processing of airborne imaging spectrometry data. Part 2: Atmospheric/ Topographic Correction, *Int. J. of Remote Sensing*, 23(13): 2631-2649.

Richter R. , D. Schläpfer, and A. Müller, 2011. Operational Atmospheric Correction for Imaging Spectrometers Accounting for the Smile Effect. *IEEE Transactions on Geoscience and Remote Sensing*, vol. 49, no. 5, p. 1772-1780.

Roberts D.A., Yamaguchi Y., and Lyon R.J.P., 1985, Calibration of airborne imaging spectrometer data to percent reflectance using field spectral measurements. In: *Proceedings of the 19th International Symposium on Remote Sensing of Environment* (Ann Arbor, MI: ERIM), pp. 295–298.

Savitzky A. and Golay M.J.E., 1964. Smoothing and differentiation of data by simplified least squares procedures. *Analytical Chemistry* 36 (8), 1627–1639.

Smith M.O, D.A Roberts, H.M Shipman, J.B Adams, S.C Willis, and A.R Gillespie, 1987: Calibrating AIS images using the surface as a reference. In R. Green, editor, In. *Proc. 3rd Airborne Imaging Spectrometer Workshop*, pages 63–69.

Vaiphasa C., 2006. Consideration of Smoothing Techniques for Hyperspectral Remote Sensing. *ISPRS Journal of Photogrammetry and Remote Sensing*, vol. 60, p. 91-99.

Acknowledgements

Ivar Barstad and Trond Loke from Norsk Elektro Optikk AS are acknowledged for providing the HySpex test data set. Amina Rangoonwala (Five Rivers Services, LLC at U.S. Geological Survey, National Wetlands Research Center) and Elijah Ramsey III, (U.S. Geological Survey, National Wetlands Research) are acknowledged for providing the Hyperion data set.